Cross-regulation and cross-talk of conserved and accessory two-component regulatory systems orchestratePseudomonascopper resistance

Sylvie Elsen, Victor Simon, Ina Attrée

Cross-regulation and cross-talk of conserved and accessory two-component regulatory systems orchestrate *Pseudomonas* copper resistance

Short title

***Pseudomonas* copper-responsive TCSs: cross-regulation and cross-talk**

Sylvie Elsen[1*], Victor Simon[1], Ina Attrée[1]

[1] University Grenoble Alpes, Institute of Structural Biology, Team Bacterial Pathogenesis and Cellular Responses, 38054 Grenoble, France

[*]Corresponding author

E-mail: sylvie.elsen@ibs.fr

Abstract

Bacteria use diverse strategies and molecular machinery to maintain copper homeostasis and to cope with its toxic effects. Some genetic elements providing copper resistance are acquired by horizontal gene transfer; however, little is known about how they are controlled and integrated into the central regulatory network. Here, we studied two copper-responsive systems in a clinical isolate of *Pseudomonas paraeruginosa* and deciphered the regulatory and cross-regulation mechanisms. To do so, we combined mutagenesis,

transcriptional fusion analyses and copper sensitivity phenotypes. Our results showed that the accessory CusRS two-component system (TCS) responds to copper and activates both its own expression and that of the adjacent nine-gene operon to provide resistance to elevated levels of extracellular copper. The same locus was also found to be regulated by two core-genome-encoded TCSs - the copper-responsive CopRS and the zinc-responsive CzcRS. Although the target palindromic sequence – ATTCATnnATGTAAT – is the same for the three response regulators, transcriptional outcomes differ. Thus, depending on the operon/regulator pair, binding can result in different activation levels (from none to high), with the systems demonstrating considerable plasticity. Unexpectedly, although the classical CusRS and the noncanonical CopRS TCSs rely on distinct signaling mechanisms (kinase-based *vs*. phosphatase-based), we discovered cross-talk in the absence of the cognate sensory kinases. This cross-talk occurred between the proteins of these two otherwise independent systems. The entire locus is part of an Integrative and Conjugative Element, and was found in other *Pseudomonas* strains where its expression could provide copper resistance under appropriate conditions. The results presented here illustrate how acquired genetic elements can become part of endogenous regulatory networks, providing a physiological advantage. They also highlight the potential for broader effects of accessory regulatory proteins through interference with core regulatory proteins.

Author Summary

Two-component regulatory systems play a key role in bacterial life by detecting and integrating a wide range of signals, allowing bacteria to continuously monitor and adapt to a changing environment. They weave a complex network with a few highly interconnected phosphorelays and numerous cross-regulations. Our study reveals connections between zinc

and copper homeostasis in a pathogenic bacterium, with cross-regulation observed for three independent, closely related transcriptional regulators, CzcR, CopR and CusR. Zinc and copper play a major role in host-pathogen interactions, and bacteria that synergize their responses to the two elements can harness a growth advantage and enhanced fitness in specific conditions. We also observed unexpected cross-talk between the core genome-encoded CopRS system and the horizontally acquired CusRS system, although the molecular control exerted by a histidine kinase on its cognate regulator differs. This plasticity observed within the two signaling systems ensures a normal regulatory response to the copper signal required to maintain copper homeostasis.

Introduction

Copper can be considered to be a heavy metal “Dr. Jekyll and Mr. Hyde”, as it is an essential trace element in biological systems but, in excess, generates free radicals with deleterious consequences [1,2]. As an antimicrobial, copper is extensively used to treat crops, to enhance breeding, and as part of medicine, with the first reports of use dating back to ancient civilizations. Human physiology exploits its properties, notably by accumulating copper in phagocytic cells and at infection sites where it contributes to protection against viruses, fungi and bacteria [3]. However, bacteria also use copper and have developed mechanisms to deal with its excess.

To maintain copper homeostasis, Gram-negative bacteria use various molecular mechanisms and machinery [1,2,4,5]. Cuproproteins are essentially extracellular or periplasmic, participating in important biological processes such as respiration, while chaperones and storage proteins capture intracellular copper cations. Copper transits from

the extracellular compartment to the cytosol, through porins or other membrane transporters. Enzymes or chemical chelators, such as glutathione, also manipulate the redox state of copper to allow chaperone loading and extrudation in case of excess. Periplasmic chaperones provide copper for cuproprotein biogenesis or deliver it to export systems. These export systems involve P1B-type ATPases or Resistance-Nodulation-Division (RND)-family multidrug efflux pumps. Periplasmic multi-copper oxidases also contribute significantly to periplasmic detoxification, by oxidizing Cu(I) to Cu(II) they reduce the metal's toxicity [2,5]. Synthesis of these molecular machines to ensure an equilibrium between cellular uptake and detoxification is mainly orchestrated by the actions of two types of regulators, MerR-like activators such as CueR that respond to cytoplasmic Cu(I), and two-component regulatory systems (TCSs) that sense periplasmic Cu(I), like the CusRS system [1,2,5]. TCSs are widespread in bacteria and play key roles in monitoring and triggering an adaptive response to environmental cues [6–8]. They comprise sensory histidine kinase (HK) proteins and cognate response regulators (RRs) communicating by phosphotransfer. Phosphorylation of RRs often results in modulation of gene expression, as most RRs are transcription factors. The copper resistance of bacterial species is also highly dependent on their genetic diversity. Indeed, additional determinants can be acquired through horizontal gene transfer (HGT), and these acquisitions tend to increase bacterial survival under copper stress [9,10]. For example, the 13-gene 37-kb GI-7 islet found in some *Pseudomonas aeruginosa* isolates was found to provide them a copper-resistant phenotype that plays a key role in bacterial colonization and persistence in hospital environments [10,11]. The accessory genes acquired are often associated with metal and/or antibiotic resistance, such as the *pco*/*sil* genes carried on the widely distributed Tn7-like structures or on the CHASRI (Copper Homeostasis and Silver Resistance Island) [9,10,12–15].

The focus of our study, *P. aeruginosa,* is a metabolically versatile Gram-negative bacterium that exhibits high resistance to copper [5]. This opportunistic animal and plant pathogen is ubiquitously present in the environment, in soil and aquatic habitats. It is one of the major causes of nosocomial infections, establishing acute and chronic infections in immunocompromized patients [16,17]. Importantly, the ability of this bacterium to cope with copper stress was shown to be essential for its pathogenicity in a mouse model [18]. Like other bacteria, *P. aeruginosa* uses several strategies and systems to resist copper poisoning and cope with varying concentrations encountered in its environment [5,19]. Expression of the copper-resistance genes is mainly orchestrated by the cytoplasmic CueR regulator and a TCS, CopRS [19,20]. The cytoplasmic Cu(I)-sensing CueR is the “first responder”, triggered after a copper shock, mainly to control genes whose products are involved in cytoplasmic copper tolerance, notably including an RND pump, the cytoplasmic chaperones CopZ1 and CopZ2, and CopA1. When high periplasmic Cu(I)/Cu(II) levels persist, the “second responder” CopR activates genes involved in periplasmic detoxification, such as *pcoAB* and *ptrA* [5]. The physiological importance of CopRS and its targets in terms of bacterial persistence and virulence has been underlined in chronic and acute wound infections [21]. Recently, the TCS DbsRS was shown to be an additional contributor to the copper response and to copper resistance [22]. CopRS responds only to copper, whereas DbsRS also responds to silver, upregulating the expression of genes involved in protein disulfide bond formation, among others. Interestingly, DbsRS requires more than 4-fold higher levels of copper for activation compared to the other two regulatory TCSs [22]. A short pulse of high copper causes a general stress response in addition to specific copper responses [20]. This general response is probably due to the generation of reactive oxygen species. In contrast, when bacteria grow in a high-copper medium, passive transport functions are downregulated to reduce membrane

114 permeability. Nevertheless, both acute and chronic high-copper conditions trigger the
115 synthesis of targets such as the tripartite RND pump CzcCBA, copper-related proteins PcoAB
116 and P-type ATPase CopA1, MexPQ-OpmE, and the three TCSs – CopRS, DbsRS, and CzcRS [20].
117 The urinary isolate IHMA87 [23], related to *Pseudomonas paraeruginosa* PA7 [24,25],
118 expresses additional, ICE-encoded TCS and copper-resistance proteins. This article reports
119 their molecular and phenotypic characterization.

120 Our results indicated that the accessory TCS is integrated into the core regulatory
121 network for copper homeostasis at *i*) the signal level, by detecting and responding to copper,
122 *ii*) the transcriptional level, as expression of its genes is controlled by several core regulators
123 responding to distinct cues, and *iii*) the molecular level, as we found cross-talk to occur with
124 non-cognate partners. Therefore, regulatory genes that accompany physiologically relevant
125 genes on mobile elements appear as an important part of the bacteria's conserved regulatory
126 network.

127

128 # Results

129 ## CusRS is a copper-responsive and strain-specific TCS

130 The two divergently transcribed operons (*IHMA87_02165-66* and IHMA87_*02164-57*)
131 present in the urinary isolate IHMA87 are reminiscent of the *copSR-copABGOFCDK* locus
132 identified in the soil-based heavy metal-tolerant β-proteobacterium *Achromobacter* sp. AO22
133 [26] (Fig 1A). These predicted operons are absent from reference strains of *P. aeruginosa*
134 (PAO1, PA14) and from taxonomic outlier PA7, the reference strain of a *P. aeruginosa* clade
135 that has recently been proposed as a new species called *P. paraeruginosa* [25]. The locus is

present in a genomic island described hereafter. The regulatory genes *IHMA87_02165-66* encode a putative copper-responsive TCS that shares homology with *P. aeruginosa* CopRS. We named this TCS CusRS due to the strong identity of the predicted proteins with the *E. coli* CusR and CusS (70.7% and 41.5% amino acid identity, respectively). For the IHMA87*_02164-57* genes, we used the "*pcoA2B2GOFCDK*" nomenclature, with "*A2 and B2*" as copies of *pcoA* and *pcoB* genes are already present in the core genome of *P. aeruginosa* and *P. paraeruginosa* (www.pseudomonas.com; [27]). The predicted operon codes for several proteins required for metal detoxification, including the multi-copper oxidase PcoA2, a putative P-type ATPase (PcoF) and copper-binding periplasmic proteins likely to play a role as chaperones (PcoC, PcoG and PcoK).

Previous DAPseq experiments showed that, *in vitro*, recombinant CusR mainly binds to the 254-bp intergenic sequence of the *cusR* and *pcoA2* genes of the IHMA87 genome [28]. The summit of the enriched DAPseq peak pointed to a perfect palindromic sequence "ATTCATnnATGTAAT" found upstream of a putative *cusR* promoter identified by BPROM (www.softberry.com) (Fig 1B). This palindromic sequence has similarities to the CopR consensus sequence in *P. aeruginosa* (CTGACAn_5GTAAT) (PRODORIC, www.prodoric.de). CusR binding to the intergenic sequence was confirmed by Electrophoretic Mobility Shift Assays (EMSA), and its specificity was demonstrated by competition with an unlabeled probe (Fig 1C), suggesting that CusR might regulate its own expression as well as that of the genes transcribed in the opposite orientation.

To assess the copper-responsiveness of the two operons and the involvement of the CusRS system in this response, we analyzed the expression of transcriptional *lacZ* reporter fusions with 500-bp sequences upstream of the *cusR* and *pcoA2* coding sequences in the wild-

type strain and the *cusR*-deleted mutant. For copper stress conditions, we exposed the bacteria to 0.5 mM $CuSO_4$ for 2.5 h. This concentration and duration do not affect bacterial viability [19]. Exposure of the wild-type strain to copper led to significant stimulation of expression of both *cusR* and *pcoA2* (Fig 1D,E). In contrast, no induction of *pcoA2* was observed following exposure of the *cusR* mutant to copper (Fig 1E), and activation of the *cusR* promoter, while still detected, was reduced about two-fold (Fig 1D). CusR therefore appears to control expression of both operons in a copper-dependent manner, but *cusR* expression must also be controlled by another copper-responsive regulatory factor.

To assess the importance of promoter elements, we constructed and analyzed a set of *lacZ* fusions associated with *cusR* upstream sequences of various lengths. Deletions affecting the palindromic sequence identified or the predicted -10/-35 boxes abolished expression, whereas a short fragment containing the palindrome maintained a copper response, but reduced both basal and activated expression levels (Fig 1D). Interestingly, mutation of a 4-bp sequence within the palindrome (ATTACATnnAT**AGCC**T) led to complete loss of the copper-responsiveness of the promoter. When examining the *pcoA2* promoter region (Fig 1E), shortening the sequence reduced the fold-change in expression following exposure to copper, whereas mutations in the palindrome led to the complete loss of copper-mediated P*pcoA2* activation. As expression of the *pcoA2* promoter is CusR-dependent, we concluded that CusR controls *pcoA2* expression by binding to the palindromic sequence identified.

To assess the extent of the *pco* operon, the mRNA levels of several genes within the locus (*pcoB2*, *pcoF*, and *pcoK*) and that of a downstream gene encoding a putative LysR-type transcription factor were measured by RTqPCR. Transcription was increased for all targets following copper stimulation, although the level of induction measured decreased with the

182 distance between the gene and the *pcoA2* promoter (S1 Fig). In all cases, interruption of *pcoA2*
183 transcription by introducing an omega interposon abolished the copper-inducing effect down
184 to *lysR*, indicating that the last gene in the locus, *lysR*, is part of the same transcriptional unit.

185 Overall, these data show that the CusRS system in IHMA87 is functional and responds
186 to copper. Following binding to a single site, CusR regulates its own expression and controls
187 the expression of the nine-gene "pcoA2" operon, which contains genes that may play a role
188 in copper resistance.

189 CusR and the *pcoA2* operon contribute to copper resistance

190 Copper concentrations in urine are known to increase during UTIs, as part of an innate
191 antimicrobial strategy [3,29]. Given the origin of IHMA87, we first questioned whether it had
192 higher copper resistance compared to three reference strains. For these reference strains, we
193 found *P. aeruginosa* PAO1 and PA14 to be more sensitive to 20 mM $CuSO_4$ than the *P.*
194 *paraeruginosa* strain PA7 (S2 Fig). In these tests, IHMA87 had the highest resistance capacity,
195 which could be provided by the additional, putative copper-resistance machinery, Pco,
196 acquired through HGT. To verify whether this was a common feature of UTI isolates, we also
197 studied two others – JT87 and TA19, which like IHMA87 are members of the PA7-like group.
198 These other strains showed variable resistance profiles, with TA19 being the most sensitive of
199 all the strains tested. Thus, high copper resistance does not appear to be a common feature
200 of UTI isolates.

201 Therefore, we investigated the role of the CusRS system and the *pcoA2* operon-
202 encoded proteins in the high copper resistance of IHMA87. First, CusR was compared to the
203 two well-described copper regulators, CopR and CueR. To do so, survival of individual, double,
204 and triple mutants was analyzed on minimal medium in the presence of high copper

concentrations (5 mM or 20 mM) and compared to that of the wild-type IHMA87 strain. As shown in Fig 2A, mutation of the *cueR* gene did not affect copper resistance whatever the genetic background, whereas the absence of CopR considerably reduced survival of the bacteria, revealing a key role of CopR and its regulon in the response to copper stress. When CopR was absent, the additional loss of CusR made the bacteria highly sensitive to copper toxicity. This sensitivity was observable at 5 mM $CuS0_4$ and accentuated at the higher concentration (Fig 2A). To determine whether this phenotype was caused by the absence of the CusR regulator *per se*, by the lack of *pcoA2-lysR* expression, or by a combined effect, we introduced in several mutants an omega interposon into the *pcoA2* gene, stopping transcription of the operon from the first gene. This interposon strongly affected the copper resistance of the Δ*copR pcoA2*::Ω strain compared to that of the Δ*copR* mutant, with an effect observable from 5 mM $CuSO_4$ (Fig 2B). Thus, the proteins encoded by the CusR-regulated *pcoA2* operon are involved in copper detoxification and resistance.

We further investigated the contribution to copper resistance of the different copper regulatory systems and the proteins encoded by the *pcoA2* operon. To do so, we followed the growth of appropriate mutant strains in lysogeny broth (LB) and compared it to IHMA87 wild-type growth. Firstly, increasing the copper concentration from 1 to 4 mM led to an extended lag phase for wild-type growth (S3A Fig). Significant cell death has been reported in the bacterial population after exposure to this high copper concentration for 2 h [19]. As the lag phase is a dynamic and adaptive period preparing bacteria for cell division, its extension indicated that more time is required both to repair altered cells and for physiological recuperation by stressed cells before exponential growth can occur [30,31]. Secondly, we observed that *cueR* and *copR* mutant growth was even more dramatically affected than wild-type growth in the presence of 4 mM $CuSO_4$. For these strains, especially Δ*copR*, the lag phase

was considerably extended (S3A Fig). This increased delay before division indicated that the copper-resistance mechanisms controlled by the two regulators are important for survival in and adaptation to the stress. Interestingly, growth of Δ*cusR* and *pcoA2*::Ω mutants was unaffected, and was similar to IHMA87 growth, indicating that these mutations had no effect on the copper resistance. In contrast, the lack of both CopR and Pco proteins completely abolished bacterial growth (S2A Fig). This result further underlined the important role in bacterial copper resistance played by the proteins encoded by the *pcoA2* operon. In the conditions used here, this role can be masked by proteins from the CopR regulon. Finally, we introduced an arabinose-inducible promoter (P*BAD*) into the chromosome, upstream of the *pcoA2* operon, and compared bacterial growth of the wild-type and modified strains over a range of copper concentrations. Increased expression of the operon conferred a clear growth advantage relative to wild-type bacteria, allowing faster adaptation to exposure to 5 mM $CuSO_4$, as indicated by the shorter lag phase (S3B Fig).

In conclusion, IHMA87 has a high intrinsic capacity to resist copper stress that can be further increased by overexpressing the *pcoA2* operon.

Three TCSs cross-regulate the *cusR-pcoA2* intergenic region

As shown in Fig 1D, copper activates *cusR* expression even in the absence of CusR. As CopR binds *in vitro* to the *cusR-pcoA2* intergenic region [28], we assessed its role as well as that of the copper-responsive regulator CueR in the residual activity of P*cusR* and that of the divergent promoter. To do so, we used transcriptional *lacZ* fusions in several genetic backgrounds lacking one, two, or all three regulators. We found that CueR was dispensable in all the conditions tested (Fig 3A, B). However, induction of *cusRS* expression was reduced in the absence of CopR compared to the wild-type background, and was lost in the Δ*cusR*Δ*copR*

mutant. This result confirmed CopR as the additional element responsible for the complete copper induction of *cusRS* in combination with CusR. Activation of the *cusRS* promoter by both CusR and CopR was abrogated by mutating the palindrome (Fig 1D), demonstrating that the same intergenic binding site is required *in vivo* for activation by both regulators.

For the expression of the *pcoA2* operon, as mentioned above, no copper induction was observed in the Δ*cusR* strain (Fig 1E, 3B). Interestingly, *pcoA2* expression was higher in Δ*copR* than in the parental strain upon exposure to copper, suggesting a negative regulatory role of CopR. In contrast, expression of *pcoA2* genes was abolished in the Δ*cusR*Δ*copR* strain, indicating that the increased activation observed in the presence of copper in Δ*copR* was the result of CusR activity (Fig 3B). This observation showed that CopR binding does not lead to transcriptional activation of the *pcoA2* promoter and, by competing for binding on the same palindrome, CopR limits access for CusR, therefore reducing *pcoA2* activation.

To further explore cross-regulation between the different pathways, we tested whether CusR affects the expression of *copA1* and *pcoA*, which are respectively regulated by CueR and CopR [19]. Expression of the *copA1* promoter was abolished in the absence of CueR, but was unaffected by deletion of either *cusR* or *copR* (Fig 3C) as expected based on *in vitro* binding data [28]. *pcoA* expression had almost the opposite profile, with no effect observed following *cueR* deletion, but a complete lack of copper-induced expression in the *copR* mutant and a slight reduction in the copper-responsiveness in the *cusR* mutant (Fig 3D). This latter result was unexpected as *in vitro* results indicate that CusR does not bind to this promoter [28]. Suspecting an indirect effect, we measured expression of P*pcoA-lacZ* and P*pcoA2-lacZ* fusions in the *pcoA2*::Ω strain. Levels of both transcriptional fusions were decreased in the presence of copper compared to levels in the wild-type strain, whereas the level of CueR-

regulated *copA* expression was similar for the two strains (Fig 3E). Based on these observations, the proteins encoded by the *pcoA2* operon may be required for the CopRS and CusRS systems to fully develop their copper-dependent activity. The effect is probably due to altered copper compartmentalization in the bacteria. These data also revealed an additional indirect layer of regulation, since the primary target of CusR, the *pcoA2* operon, seems important for both TCSs to mount a copper response.

Mining and reanalyzing the DAPseq data [28] indicated that three other RRs strongly targeted the *pcoA2-cusR* intergenic sequence centered at the same position (S4A Fig). These RRs are the two poorly characterized regulators IrlR and MmnR, and the well-known zinc-responsive protein CzcR that binds to the sequence "GAAACn_6GTAAT" [32]. Additional target genes were found to be shared by CopR, CusR and CzcR (S4B,C Fig), presumably due to the extensive similarity of their consensus sequences, especially the second half-site "GTAAT". Therefore, we analyzed the roles of these additional RRs on the expression of both the *cusRS* and *pcoA2* operons.

The TCS CzcRS is known to respond to several signals, including zinc stress [33]. We therefore assessed its effect on *pcoA2* and *cusRS* expression in the presence of copper and/or zinc. As a control of CzcR activity, we introduced a P*czcC-lacZ* fusion into the wild-type and Δ*czcR* strains, as a known CzcR target. Fig 4 shows that, as expected, the *czcC* promoter was upregulated after the addition of zinc, with or without the addition of copper, and that this upregulation was CzcR-dependent. Furthermore, the expression of *pcoA2* was activated by zinc to almost the same level as by copper. Exposure to both stimuli was slightly, but significantly, more efficient. Zinc activation was lost in the absence of CzcR, and the *pcoA2* expression level dropped to that observed in the wild-type in the presence of copper alone

(Fig 4). Therefore, both CusR and CzcR control and activate expression of the *pcoA2* operon to similar extents. A distinct expression profile was observed for the *cusR* promoter: while copper strongly activated its expression, the induction following exposure to zinc was lower. In addition, zinc bypassed the copper effect when bacteria were simultaneously exposed to both metals. In the absence of CzcR, this "restraining" effect was lost, and the high-copper-inducible effect was restored, suggesting that CzcR must conceal the CusR binding site.

We then assessed a potential regulatory role of MmnR and IrlR and observed no *mmnR* or *irlR* deletion phenotypes in terms of *pcoA2* operon and *cusR* expression, even in the presence of copper (S6 Fig). However, we cannot exclude that this was due to an absence of signal and activation of the sensor in our experimental conditions.

Overall, the data indicate that *cusRS* and *pcoA2* operons are controlled *in vivo* by at least three TCSs: CusRS, CopRS, and CzcRS. The three RRs bind to the same palindromic site but modulate expression of the divergent operons differently. Indeed, while CusR and CzcR activate both operons, even if the latter is less effective on the *pcoA2* promoter, CopR only activates *cusRS*, repressing the *pcoA2* operon by hindering the positive action of CusR (S7 Fig).

Molecular cross-talk between the CopRS and CusRS systems

The *P. aeruginosa* CopRS system works in an unusual way [34]. Instead of relying on a conventional "phosphorylation-based mechanism" where the sensor allows the phosphorylation of the response regulator upon detecting a signal, CopS displays phosphatase activity toward CopR. Exposure to copper thus relieves the inhibition by allowing CopR to activate its target genes. The mechanism leading to phosphorylation of CopR remains unidentified. We confirmed the "phosphatase-based mechanism" of the CopRS system in the *P. paraeruginosa* strain IHMA87, as demonstrated in Fig 5A. Indeed, in a *cusRS* background,

the absence of CopS led to a high-copper-blind expression of *pcoA*, whereas constitutive phosphatase activity of the sensor $CopS_{His235A}$ mutation abolished *pcoA* expression. The same pattern was observed for *cusR* expression (Fig 5A). This result also confirmed that CopR can activate expression of this promoter in a Δ*cusRS* background, as previously suggested by the data presented in Fig 3A.

We then analyzed the functioning of the CusRS system in a genetic background lacking the CopR and CopS proteins to avoid any protein interference. As shown in Fig 5B, neither *pcoA2* nor *cusRS* operons were activated in the strain lacking the sensor protein CusS. This result indicates both that this HK is required for CusR activation by phosphorylation, and that no other protein can phosphorylate CusR. We also confirmed that the phosphorylated form of CusR is the active form, because no gene expression was observed when its conserved phosphorylation site (Asp_{54}) was mutated to an alanine (Fig 5B). In addition, mutation of the autophosphorylation site of CusS (His_{266}) abolished the expression of the two operons, indicating that it is required for the system to function properly (autophosphorylation prior to phosphotransfer). Altogether, these data show that the CusRS system is a canonical TCS, functioning like the *E. coli* CusRS system, with the detection of a signal triggering a phosphorylation cascade ultimately leading to target gene activation.

The two TCSs were then studied in different combinations of mutants of their HK gene to obtain information on possible cross-talk between non-cognate HKs and RRs. The results are summarized schematically in S7 Fig. Focusing on a CopR-only-activated promoter, we found that deletion of *copS* led to an identical copper response pattern of P*pcoA*-*lacZ* expression to that observed in the wild-type strain or in a strain lacking the *cusS* gene (Fig 5C). However, deletion of both *copS* and *cusS* led to the strong constitutive activation of P*pcoA*

(copper-blind expression) that was observed in the Δ*copS* mutant in the absence of CusRS (Fig 5A). This result indicates that the HK CusS can compensate for an absence of the HK CopS, controlling CopR activity in the absence of the cognate partner. Thus, like CopS, CusS could act as a CopR phosphatase to prevent gene expression in the absence of copper when its cognate partner is absent. Alternatively, interaction between CusS and CopR in the absence of CopS might prevent phosphorylation of CopR in the absence of signal. We further observed that control of CopR by CusS does not require its cognate HK to be absent. Indeed, normal expression of P*pcoA* was observed when the constitutive phosphatase $CopS_{H235A}$ was produced (Fig 5C), indicating that CusS permits CopR phosphorylation following detection of copper.

To determine whether CopS could also interact with CusRS, we used P*cusR-lacZ* (Fig 5D) and P*pcoA2-lacZ* (Fig 5E) transcriptional fusions in several mutant genetic backgrounds. As expected, absence of *copS* had little effect on the two promoters: indeed CusS could control the phosphorylation status of CusR and of CopR, as observed above, and both these proteins activated transcription only in response to the copper signal. However, when *cusS* was deleted, in the absence or presence of copper, a slight increase in P*cusR* expression levels was observed (Fig 5D), and the effect on P*pcoA2* expression was even more pronounced (Fig 5E). Transcriptional activation could be attributed to activity of phosphorylated CusR as the signal was lost when $CusR_{D51A}$ was synthesized in the Δ*cusS* background mutant. Thus, CopS appears to permit CusR phosphorylation in the presence of copper, but also in its absence, and to control its phosphorylation status, although not as tightly as the cognate HK CusS. P*cusR* activation was not observed in the $CopS_{H235A}$Δ*cusS* strain, supporting the need for CopS for phosphorylation of CusR (Fig 5D). Copper-blind expression of both P*cusR* and P*pcoA2* was then observed in the Δ*cusS*Δ*copS* mutant. As CusR cannot be

368 phosphorylated in bacteria lacking both sensors (CusS and CopS), the P*cusR* expression
369 pattern observed (Fig 5D) can be attributed mainly to dysregulated CopR activity (Fig 5C).
370 However, high levels of unphosphorylated CusR also contributed to these activities as the
371 copper-blind expression of P*cusR* noticed in $CusR_{D514A}$Δ*copS*Δ*cusS* was still observed, albeit to
372 a lesser extent (Fig 5D). This unphosphorylated CusR activity was clearly observed on CusR-
373 only-activated *pcoA2* promoter in Δ*cusS*Δ*copS* that displayed copper-blind expression (Fig 5E):
374 as expected, similar activity levels were then observed when the CusR phosphorylation site is
375 mutated in the double mutant background ($CusR_{D514A}$Δ*copS*Δ*cusS*) (Fig 5E). Furthermore,
376 P*pcoA2* expression levels were lower in Δ*cusS*Δ*copS* compared to in Δ*cusS,* which underscores
377 the negative effect of phosphorylated CopR binding to the promoter (Fig 5E). In the
378 $CopS_{H235A}$Δ*cusS* background, the *pcoA2* promoter was not expressed, as no CusR is synthesized
379 (Fig 5D).

380 Finally, we wondered whether the CopRS and CusRS systems respond to and modulate
381 their regulon within the same range of copper concentrations. We compared their individual
382 sensitivities to copper and their sensitivity relative to that of the cytoplasmic detector CueR.
383 To do so, we used *lacZ* fusions to monitor the expression of a specific target of each
384 transcriptional regulator over time in response to different copper levels. We found CopRS
385 and CusRS to display a similar sensitivity and response to copper, inducing their target in the
386 presence of 0.5 mM $CuSO_4$. In contrast, CueR activates its target at lower copper
387 concentrations (from 0.01 mM) (S8 Fig).

388 To conclude on cross-talk, not only do the CopRS and CusRS systems share similar DNA-
389 binding sites and a target sequence, their HK can compensate for each other, with higher
390 efficiency observed for CusS.

Horizontal acquisition of the *cusRS* and *pcoA2* operons

As mentioned above, the reference *P. paraeruginosa* strain PA7 lacks the *cusRS* and *pcoA2* operons. Analysis of the genomic environment surrounding this copper-related locus showed that it is present on a genomic island that presents the features of an Integrative and Conjugative Element (ICE) (Fig 6A). ICEs are large mobile genetic elements that are crucial for the genetic plasticity of bacteria [35,36]. Consequently, the copper-related locus was probably acquired by HGT. We named this island ICE1_IHMA, and it is one of three predicted ICEs in the IHMA87 genome. It is 96,269 bp long, inserted at a tRNA-Gly site, and has an average GC content of 64%. Among the 100 predicted coding sequences present on ICE1_IHMA, some correspond to core ICE genes, required for the element's life cycle. These include signature genes coding for an integrase of phage origin (*int*) and a MOB(H)-type relaxase [37]. In addition, the element possesses a set of mating-pore formation (MPF) genes encoding a T4SS (*tfc* genes) including an ATPase (*tfc16/virB4*) and a Type IV coupling protein (*tfc6/t4cp2*). Among the eight types of MPF system – classed based on diverse features – ICE1_IHMA is a type G (MPF_G). These systems are frequently found in Proteobacteria [38]. ICEs also carry specific cargo genes, which usually provide the host with benefits and diverse phenotypic properties [35]. Based on sequence homology and the organization of its core genes, ICE1_IHMA is highly similar to PAGI-2, a prevalent *clc*-like family ICE in *P. aeruginosa* [16] (Fig 6A). By comparison with PAGI-2, we defined two specific cargo modules in ICE1_IHMA, named A and B. Module A comprises four genes, of which three (*IHMA87_02154-52*) are predicted to encode a CzcCBA-type heavy metal RND efflux pump. To assess whether this pump could be involved in copper efflux, we deleted *IHMA87_02154-52.* No effect was observed in terms of survival of the mutant obtained upon exposure to a high copper concentration (S2 Fig). In line

414 with this result, the promoter region of *IHMA87_02154-52* was not targeted *in vitro* by CusR
415 or CopR [28]. The other module, Module B is composed of 21 cargo genes, among them the
416 *cusRS* and *pcoA2* operons, but also several genes predicted to be involved in resistance to
417 chromate and arsenic compounds. Copper, arsenic, and chromium resistance genes
418 frequently co-occur in mobile genetic elements, favoring the spread of both metal resistance
419 genes and antibiotic resistance. The spread of such resistance is of concern because co-
420 selection promotes the acquisition of antibiotic resistance [10,39]. Although the gene
421 encoding the LysR-type regulator is present on PAGI-2, it was considered to be part of Module
422 B, since we demonstrated that it was part of the *pcoA2* operon.

423 As ICEs are modular and cargo genes can be exchanged, we assessed how the two cargo
424 modules are distributed in bacterial genomes by performing blast searches against the NCBI
425 database (Fig 6B). Modules A and B from ICE1_IHMA are both present in several bacteria from
426 various genera. The most frequently represented genus was *Pseudomonas*, and the
427 corresponding predominant species are *aeruginosa* and *paraeruginosa*. The two modules
428 were also identified in other genera with distinct distributions, for example in a few
429 *Achromobacter* and *Stenotrophomonas* genomes, whereas only Module A was identified in
430 some *Comamonas* genomes. Interestingly, if the *lysR* gene located at the 3' extremity of the
431 *pcoA2* operon is excluded from the search for Module B, identical results were obtained. This
432 further emphasizes its co-occurrence with the *cusRS* and *pcoA2* operons, and suggests a
433 possible role in their regulation.

434 We next focused our analysis on the distribution of the region from *lysR* to *cusS*, which
435 comprises the entire sequence of the two operons (Fig 6B). Initially, the search provided more
436 hits than obtained for searches with the whole of Module B, suggesting that this region can
437 be acquired or maintained independently of the rest of the module. The genera harboring the

438 locus were similar to those with the module B, but the distribution varied with a higher ratio
439 of *Pseudomonas*. Among species, the region was mostly represented in *P. aeruginosa* and
440 *P. paraeruginosa*, with only two strains of *Pseudomonas* not belonging to these species. We
441 then examined the distribution and conservation of the *lysR-cusS* region over a database of
442 494 complete *P. aeruginosa* and *P. paraeruginosa* genomes. The clades were named based on
443 the approach described by Freschi *et al.* [40] from 1 to 5, and, as proposed by Rudra *et al*. [25],
444 outlier group 3 was (re)classified as *P. paraeruginosa* (*P.p*). Bioinformatics analysis revealed
445 the locus to be present in several strains of *P. aeruginosa* clades 1 and 2*,* and (as expected) in
446 the IHMA87 strain, which is classed in clade 3 (Fig 6C). The locus was not detected in the few
447 clade 4 and 5 strains for which genomes are available (www.pseudomonas.com; [27]).The
448 locus was present as part of a putative ICE in over 80% of genomes. In the remaining 20% of
449 genomes, it was part of regions bearing some similarity to an ICE, as determined based on
450 neighboring genes and their predicted functions. The reason these regions were not
451 immediately predicted to be ICEs can be attributed either to ICE degeneracy, or to a detection
452 failure. In all the loci identified, the motif recognized by CusR in the *pcoA2-cusRS* intergenic
453 sequence was conserved, indicating that the copper-resistance genes can be integrated into
454 the bacterial regulatory network, allowing them to be readily expressed in their host under
455 appropriate conditions.

456 Taken together, these data show that the *lysR-cusS* locus involved in copper resistance
457 is mainly found in the *Pseudomonas* genus where it can be acquired by HGT as part of an ICE.
458 As demonstrated by our research, the integration of this locus into the regulatory network
459 involves cross-regulation and cross-talk with endogenous regulatory actors. These constraints
460 must limit the acquisition of the locus by other genera.

Discussion

In this study, we examined the integration of an acquired copper-resistance locus into a housekeeping system, both at the level of regulatory pathways and in terms of the protection it affords against toxic copper concentrations. The ICE-encoded copper-responsive TCS CusRS was shown to control expression of its own gene and a divergently transcribed nine-gene operon, *pcoA2B2GOFCDK-lysR*. The copper-related elements described here were initially acquired by HGT, and are not the only example of accessory copper genes found in *P. aeruginosa* species [11]. In bacteria, acquired systems can be even more efficient in coping with copper stress than the core mechanisms, as observed for the *copXL* locus in *Staphylococcus aureus* [41]. Although capable of conferring bacterial copper resistance, the results presented here showed that the positive effects of the *P. paraeruginosa* Pco proteins are masked by those of the core copper homeostasis proteins, controlled by the CopRS system [19]. However, mutation of the *pcoA2* operon reduced the metal response of both the CopRS and the CusRS regulatory systems (Fig 2B): this indicates that Pco proteins also play a role in maintaining copper compartmentalization that affects signal detection by both acquired and conserved sensory HKs. Our results showed that the *pcoA2* operon contributes to overall copper homeostasis as it is under the control of the main core TCS CopRS. The control of accessory genes by housekeeping TCSs has previously been documented for copper homeostasis regulation. For example, in *E. coli*, although chromosome-encoded CusRS and plasmid-borne PcoRS systems are independent TCSs, CusR activates expression of the plasmid-encoded *pcoE* gene [42]. Similarly, in emerging pathogenic *S. aureus* strains, the core-encoded regulator CsoR controls expression of genes present in several mobile elements, conferring a phenotype that is hyper tolerant to copper [41,43]. In the *P. paraeruginosa* strain

484 studied here, we found CopR to downregulate expression of the *pcoA2* operon, probably by
485 competing with CusR for DNA binding (Fig 3B). This finding was unexpected as the *pcoA2*
486 operon does not appear to be a poisoned gift, given that it can improve the bacteria's
487 resistance to copper stress when artificially overexpressed.

488 Although the homologous CopRS and CusRS systems respond to the same molecule
489 over the same concentration range, their downstream signaling mechanisms differ. The HKs
490 are often bifunctional enzymes with both phosphatase and autokinase activities, differentially
491 triggered depending on the signal detection [44]. We confirmed that the CopRS system relies
492 on a "phosphatase mechanism" in *P. paraeruginosa* like that observed in *P. aeruginosa* [34],
493 where CopS dephosphorylates CopR. The copper signal shuts down the phosphatase activity
494 of CopS and, consequently, CopR becomes active, triggering gene expression. With this *modus*
495 *operandi*, absence of HK leads to a copper-blind activation of the CopR regulon [34]. In the
496 strain studied here, the CusRS system acted like a canonical TCS, functioning more like the
497 recently discovered copper-responsive DbsRS TCS in *P. aeruginosa* [22]. DsbS can
498 dephosphorylate its partner DsbR and, upon direct binding of copper, it can
499 autophosphorylate. The phosphate is subsequently transferred to DsbR, which in turn
500 activates target genes, notably those responsible for copper resistance [22]. Although no CusR
501 dephosphorylation was observed, the data indicated that CusS HK could dephosphorylate the
502 non-cognate CopR in the absence of CopS.

503 The *P. paraeruginosa* IHMA87 proteins CusR and CusS share 70.7% and 41.5%
504 sequence identity, respectively, with their *E. coli* homologs [27]. In addition, both CusR
505 regulators have a perfectly palindromic DNA-binding site and a very restrictive regulon [42].
506 Only one significant target sequence was identified for IHMA87 CusR by DAPseq [28]. This

sequence is the palindrome "ATTCATnnATGTAAT", located in the intergenic sequence *pcoA2-cusR*. It is perfectly conserved in the equivalent locus in *Achromobacter* sp. AO22 [26]. *E. coli* CusR preferentially binds to the palindrome "AAAATGACAAnnTTGTCATTTT" [42], located between the two divergent operons *cusRS* and *cusC(F)BA*. Although no other chromosomal binding site could be identified [45], *E. coli* CusR also directly controls expression of the plasmid-borne gene *pcoE*, which has palindromic sequence (TGACAAnnTTGTCAT) in its promoter. Another feature of the *E. coli* CusRS system is its ability to confer resistance to silver toxicity. Thus, the HK CusS was shown to bind to both copper and silver [46,47]. As observed for chromosomally-encoded CusRS and plasmid-encoded PcoRS systems in *E. coli* [42], CopRS and CusRS are independent systems. However, in addition to the known cross-regulation (at the level of both gene target and signal) [44], we demonstrated *in vivo* molecular communication between the unrelated HK-RR pairs. Variable levels of cross-talk within TCS signaling pathways have also been reported in other bacteria, ranging from absent (or not observed) to highly represented as in the case of *Mycobacterium tuberculosis* [48,49]. As TCSs often arose during evolution through gene duplication, the high levels of sequence identity shared by the paralogs may favor interactions. However, distinct mechanisms normally evolve rapidly after duplication to insulate the systems, preventing inappropriate interactions and favoring the specificity of the molecular interactions within each system. Although generally considered to be a disadvantage for the bacteria, as it decreases the specific response and may trigger inappropriate responses, cross-talk can also be beneficial. Indeed, it can provide some evolutionary benefits, such as complex signal-processing mechanisms or priming to respond to future stimuli [44,49,50]. In the IHMA87 strain, our results indicate that CusS could compensate for the absence of CopS by maintaining the relevant CopR phosphorylation status thanks to its copper-responsive function. CusS could also control CopR activity in the presence

of the constitutive phosphatase $CopS_{H235A}$ (Fig 5C). The reciprocal reaction was less efficient, as CopS was only partially capable of replacing CusS in its interaction with CusR. Whether the system also controls CusR phosphorylation is less clear, as this reaction requires a phosphotransfer step not reported for the CopS-CopR pair. In addition, results were blurred by cross-regulation exerted by the two TCSs on target genes (Fig 5D,E). We nevertheless produced schematic models that fitted the *in vivo* results indicating the cross-talk between CusRS and CopRS (S7 Fig). These models will need to be consolidated by further experiments, in particular to determine the extent of the protein interactions and the HK activities toward the cognate/non-cognate RRs.

The *in vivo* cross-talk detected between the CusRS and CopRS systems in *P. paraeruginosa* was unexpected. First, CopRS is encoded by the core genome of the bacterium whereas CusRS is coded by genes present in the HGT-acquired ICE. Second, while the RRs of the two systems share 69% sequence identity, the HKs CopS and CusS only share 36.4% identity. These two HKs also act differently on their cognate RRs. Third, cross-talk usually involves the absence of both the reciprocal RR and the cognate HK of two distinct TCSs, as observed for CpxA–CpxR and EnvZ–OmpR in *E. coli* and mentioned for cross-talk from CusS to OmpR and CpxR [44,50]. The reason is that the RRs usually compete with other RRs for interaction with their cognate partner(s) to prevent misregulation. However, here, in the absence of CopS, CusS controlled the activity of CusR and CopR normally. Moreover, it did so even in the presence of the constitutive phosphatase $CopS_{H235A}$. Although it originated from a lateral transfer, our bioinformatics analyses revealed that the locus is mainly present in *P. aeruginosa* and *P. paraeruginosa* strains, where the genes are probably readily expressed. The expression advantage of copper resistance on bacterial fitness might explain this distribution. In addition, the cross-regulation and cross-talk with endogenous regulatory TCSs

may be required for appropriate integration of the locus, making it possible to tightly control expression without creating a burden. This would naturally limit spread of this ICE to other species.

Despite having been acquired by HGT, we also observed that the *cusRS-pcoA2* locus was a site of fierce competition for regulation, completely integrated into the conserved TCS regulatory network. Indeed, four core genome-encoded RRs – IrlR, MmnR, CzcR and CopR – in addition to the accessory CusR can bind the *cusRS-pcoA2* intergenic region *in vitro* [28]. All these RRs belong to the OmpR family with winged-HTH effector domains. The corresponding genes are organized in a two-gene operon with downstream, overlapping genes encoding the cognate HK (www.pseudomonas.com; [27]). Phylogenetic analysis clustered them together, inferring that they emerged by RR-HK pair duplication [51]. A genome-wide binding assay revealed these closely related regulators to share similar DNA-binding motifs, and extensively overlapping gene targets (Fig S4) [28]. The physiological relevance of IrlR and MmnR binding could not be assessed here, as the signals detected by their cognate HK are as yet unknown. Although the *mmnRS* locus was reported to be upregulated in response to copper shock [52], we observed no effect of *mmnR* inactivation on the expression of *cusRS* and *pcoA2* in the presence of copper (S5 Fig).

Even if the five RRs bind to similar targets *in vitro*, their physiological role is more delimited, as CopR, CusR and CzcR are known to have their own regulon with only a few shared and cross-regulated targets. Similarly, in *Pseudomonas stutzeri*, comparison of the *in vitro* binding sites and regulons of CzcR and the paralogs CopR1/CopR2 revealed limited target sharing and cross-regulation [53]. In addition, their binding was shown to induce either activation or repression with response amplitudes varying depending on the promoter bound

578 [53]. Along the same lines, while CusR, CopR and CzcR could bind to the same DNA region, we
579 observed that their effects on the expression of *cusRS-pcoA2* ranged from activation (to
580 various extents) to no activation at all (illustrated in S6 Fig). The molecular dynamics of the
581 TCSs, signal perception by HKs, and phosphorylated RR levels are among other important *in*
582 *vivo* parameters that will need to be investigated. Nevertheless, based on the results
583 presented here, these variable outcomes may also be due to differences in RR-DNA and/or
584 RR-RNA polymerase interaction, as demonstrated for the *E. coli* paralogs KdpR and OmpR [54].
585 Indeed, a new set of target genes for duplicated RRs can evolve through changes in the DNA-
586 binding sites recognized and their capacity to interact with the RNA polymerase [55].
587 However, sometimes the second mechanism is not without consequences, as shown here,
588 where CopR not only fails to activate *pcoA2* promoter expression, but actually inhibits it by
589 competing with CusR for binding. Furthermore, as proposed for CopRS and CzcRS in *P. stutzeri*
590 [53], we cannot exclude the possibility that cross-talk between these two homologous TCSs
591 exists, adding a level of complexity to the regulatory networks. Overall, our findings
592 emphasized that the effects of a regulator binding to a promoter cannot always be predicted
593 and must be determined on a case-by-case basis.

594 This study also illustrated the connection between zinc and copper homeostasis, with
595 cross-regulation observed with CzcR, CopR and CusR. The two metals play a major role in host-
596 pathogen interactions and, during infection, higher copper and zinc concentrations can be
597 encountered by bacteria under the same physiological conditions. For example, in
598 phagolysosomes [56], these two metal ions contribute to bacterial killing. Synergized
599 responses to the two elements relying on cross-regulation have been described in *P.*
600 *aeruginosa* [57,58]. For instance, high copper concentrations lead to both increased zinc and
601 copper resistance, and overproduced CopR can activate expression of *czcRS*, which in turn

602 activates CzcCAB synthesis [57]. The regulator CzcR also controls the expression of the CopR-
603 regulated *ptrA-czcE-queF* operon [33,58]. In a previous study, we found that PtrA is a
604 periplasmic protein involved in copper tolerance [59]. In addition, CzcE was recently found to
605 be a novel element required for zinc resistance [33]. Therefore, this operon harbors genes
606 involved in tolerance to both metals. The data presented here further demonstrated that CzcR
607 activates expression of the *pcoA2* operon, which is integrated in the RR regulon. As CzcRS is
608 known to respond to cadmium in addition to zinc [33], this broadens the range of signals
609 capable of triggering expression of the *pcoA2* and *cusRS* operons.

610 In conclusion, some *P. aeruginosa* strains harbor ICE carrying genes for copper
611 resistance, as well as cognate regulatory elements that are completely integrated into the
612 bacterial regulatory network. Synthesis of this accessory copper system is tightly controlled in
613 the intergenic regulatory region, which is a hot spot for binding of five RRs. The RRs compete
614 for DNA binding and their docking stimulates or silences gene expression. The reason for the
615 negative effect exerted by the regulator CopR is not known, but expression of the *pcoA2*
616 operon can be modulated by signals other than copper. Therefore, the accessory copper-
617 resistant mechanisms might be physiologically relevant in (as yet unidentified) conditions
618 encountered in the host or in the environment.

619

620 # Material and Methods

621 ## Bacterial strains and growth conditions

622 The *E. coli*, *P. aeruginosa* and *P. paraeruginosa* strains used in this study are described
623 in S1 Table. Bacteria were grown aerobically in LB at 37 °C with agitation. To assess the effect

of copper on gene expression, overnight cultures were diluted to an OD_{600} of 0.1 in LB supplemented with the indicated $CuSO_4$ concentrations, and growth was continued until the OD_{600} reached around 1.0 (2.5 h). Growth in 96-well plates at 37 °C with agitation was assessed by following the OD_{595} of 200-µL cultures in LB with the $CuSO_4$ concentrations indicated. Plates were read by a microplate reader at the indicated times. For copper sensitivity plate assays, 15 g/L agar was added to M9 minimal medium (48 mM Na_2HPO_4, 22 mM KH_2PO_4, 9 mM NaCl, 19 mM NH_4Cl, 2 mM $MgSO_4$, 0.1 mM $CaCl_2$, 0.2% Glucose) supplemented with $CuSO_4$. When LB cultures reached OD_{600} of 1.0, 10 µL of a 10-fold serial dilution of the cultures were spotted on the M9 media and the plates were incubated for 1 to 2 days at 37 °C. Antibiotics were added at the following concentrations (in µg/mL): 200 spectinomycin (Sm), 100 ampicillin (Ap), 50 gentamicin (Gm), 10 tetracycline (Tc), and 10 chloramphenicol (Cm) for *E. coli*; 75 Gm and 75 Tc in presence of 5 irgasan (Irg) in LB for *P. aeruginosa*.

Plasmids and genetic manipulation

The plasmids used and the primers for PCR are listed in S1 and S2 Tables, respectively. All constructions were verified by sequencing.

To generate *P. paraeruginosa* deletion mutants, upstream (sF1/sR1) and downstream (sF2/sR2) flanking regions of the different genes were fused and cloned into an *Sma*I-cut pEXG2 plasmid by sequence- and ligation-independent cloning (SLIC) using the appropriate primer pairs [60].

For chromosomal insertion of the P*BAD* upstream *pcoA2* operon, a pEXG2 plasmid was created by SLIC with upstream and downstream sequence of the *pcoA2* promoter sequence, creating a *Spe*I site 52 bp upstream of the start codon. Then, the 1580-bp "*araC*-P*BAD*"

fragment was excised from pSW196 using *Xba*I and cloned into the *Spe*I site created, to produce pEXG2-P*BAD-pcoA2*-Sp.

For mutagenesis by insertion of the Ω interposon, the MCS-contained *Bam*HI site was first deleted from pEXG2 (pEXG2ΔB). Then a *de novo Bam*HI site was created while using SLIC to fuse two fragments of *pcoA2* in *Sma*I-cut pEXG2ΔB. Finally, the Ω interposon from pHP45Ω was introduced into *Bam*HI-cut pEXG2ΔB-*IHMA_02164*.

To replace residue His by Ala in CusS and CopS, we used SLIC to generate a fragment with the mutated codon and create a *Sac*II site to allow subsequent restriction analysis screening of PCR-amplified fragments.

To create the transcriptional *lacZ* fusions, the miniCTX-*lacZ* plasmid was first modified to prevent transcriptional interference by integrating the strong *rrnB* terminator sequence into its *Xho*I-*Kpn*I sites, as described in Trouillon *et al.* [61], to produce miniCTX-T*rrnB*-l*acZ*. Then, fragments comprising the ATG and around 500 bp upstream of each target analyzed were amplified using the appropriate pairs (sF/sR) for insertion into *Sma*I-cut miniCTX-T*rrnB*-*lacZ* by SLIC. To create mutations in the regulator binding sites, another pair of overlapping mutated primers (sR1/sF2) were used to create two overlapping fragments (sF/sR1 et sF2/sR), also inserted into *Sma*I-cut miniCTX-T*rrnB*-*lacZ* by SLIC.

The pEXG2- and miniCTX-T*rrnB*-*lacZ*-derived vectors were transferred into *P. paraeruginosa* IHMA87 strains by triparental mating using the helper plasmid pRK600. Allelic exchanges for mutagenesis were selected as previously described [62]. To create the mutant encoding the $CusR_{D51A}$ protein, the mutated sequence was introduced into the Δ*cusR* mutants to replace the deleted gene.

669 For *E. coli* overproduction of CusR protein with an N-terminal 6xHis-Tag, the *cusR* gene
670 was first amplified by PCR using IHMA87 genomic DNA as template, and SLIC was used to
671 insert the fragment into the pET15b plasmid cut with *Nde*I and *Bam*HI.

672 ## β-galactosidase activity assay

673 β-galactosidase activity was assessed at least in triplicate as previously described
674 [63,64], after 2.5 h of growth in the indicated media. On the bar graphs, activities were
675 expressed in Miller Units (MU), and error bars correspond to the standard error of the mean
676 (SEM). When relevant, statistical significance was assessed using ANOVA test with Tukey's
677 method.

678 ## Reverse Transcription-quantitative Polymerase Chain Reaction (RTqPCR)

679 Extraction of total RNA, cDNA synthesis and qPCR were carried out as previously
680 described [61] with the following modifications: the cDNA was synthesized using 3 µg of RNA
681 and the SuperScript IV first-strand synthesis system (Invitrogen). For each strain and condition,
682 mRNA expression was measured for three biological replicates. Data were analyzed with the
683 CFX Manager software (Bio-Rad), and expression levels were normalized relative to *rpoD*
684 reference Cq values using the Pfaffl method. The sequences of the primers used can be found
685 in S2 Table. Statistical analyses were carried out with *T*-test.

686 ## Production and purification of CusR

687 His_6CusR (H_6CusR) was produced in *E. coli* BL21 Star (DE3) strains harboring pET15b-
688 CusR, grown in LB at 37 °C. Expression was induced by adding 1 mM isopropyl β-D-1-
689 thiogalactopyranoside when cultures had reached an OD_{600} of 0.6. Cells were grown for a
690 further 2 h at 37 °C and 150 rpm, and then harvested by centrifugation. They were

resuspended in 20 mL of IMAC buffer (25 mM Tris-HCl, 500 mM NaCl, pH 8) containing 10 mM Imidazole and supplemented with Protease Inhibitor Mixture (Complete, Roche Applied Science) for lysis at 4 °C by sonication. After centrifugation at 200,000 × g for 30 min at 4 °C, the soluble fraction was loaded onto a 1-mL anion exchange column (HiTrap 1 mL HP, GE Healthcare) and purified on an Akta purifier system. The protein was eluted by applying a 30-mL gradient ranging from 10 to 200 mM Imidazole in IMAC buffer at a flow rate of 1 mL/min. Eluted protein was diluted 1:20 in Tris-NaCl buffer (50 mM Tris- HCl, 150 mM NaCl, pH 8) for conservation before use.

Electrophoretic Mobility Shift Assays (EMSA)

Probes were generated by annealing complementary primer pairs, one of which was Cy5-labeled, to form the fluorescent probe. 0.5 nM of the resulting 60-bp DNA fragments were incubated for 15 min at 25 °C in EMSA Buffer (20 mM HEPES, 80 mM KCl, 20 mM $MgCl_2$, 0.8 mM EDTA, glycerol 7.5%, 0.1 mM dithiothreitol, pH 7.9). For competition assays, unlabeled DNA probes were added to the reaction at either 0.5 nM (equal amount) or 200 nM (400-fold excess). The proteins were then added at the indicated concentrations in a final reaction volume of 20 µL and incubated for a further 20 min at 25 °C. Samples were then loaded onto a native 5% Tris-Borate-EDTA (TBE) polyacrylamide gel and run at 100 V and 4 °C in cold 0.5X TBE Buffer. Fluorescence imaging was performed using an ImageQuant 800 imager.

Bioinformatics analyses

ICEs were identified and delineated using the web-based tool ICEfinder [65]. ICEs were typed using ConjScan [66] on the Pasteur Galaxy platform [67]. Sequences were aligned and visualized with clinker [68]. Blast analyses were performed with BLASTn [69]. Complete

714 genome sequences of *P. aeruginosa* (n= 487) and *P. paraeruginosa* (n=7) were downloaded
715 from the Pseudomonas Genome Database [27]. Genomes were annotated with Prokka [70],
716 and core genomes were determined with Roary [71] before alignment with MAFFT using the
717 default parameters [72] on the Galaxy server [73]. The resulting alignment was used to build
718 a maximum-likelihood phylogenetic tree with FASTTREE [74] on the Galaxy server. The
719 phylogenetic tree was finally visualized and annotated using iTOL [75].

720

721 Acknowledgments

722 We thank Eric Faudry for valuable advice on protein purification and Emmanuel
723 Thévenon for giving us access to the ImageQuant imager. *P. aeruginosa* IHMA87 was obtained
724 from the International Health Management Association, USA. This work was supported by
725 GRAL, funded through the University Grenoble, Alpes graduate school (Ecoles Universitaires
726 de Recherche) CBH-EUR-GS (ANR-17-EURE-0003). We further acknowledge support from
727 CNRS, CEA and Grenoble Alpes University. Victor Simon's Ph.D. fellowship was funded by the
728 French Ministry of Education and Research.

729 References

730 1. Argüello JM, Raimunda D, Padilla-Benavides T. Mechanisms of copper homeostasis in bacteria.
731 Front Cell Infect Microbiol. 2013;3. doi:10.3389/fcimb.2013.00073

732 2. Andrei A, Öztürk Y, Khalfaoui-Hassani B, Rauch J, Marckmann D, Trasnea P-I, et al. Cu
733 Homeostasis in Bacteria: The Ins and Outs. Membranes (Basel). 2020;10: 242.
734 doi:10.3390/membranes10090242

735 3. Focarelli F, Giachino A, Waldron KJ. Copper microenvironments in the human body define
736 patterns of copper adaptation in pathogenic bacteria. PLoS Pathog. 2022;18: e1010617.
737 doi:10.1371/journal.ppat.1010617

738 4. Rensing C, Grass G. *Escherichia coli* mechanisms of copper homeostasis in a changing
739 environment. FEMS Microbiol Rev. 2003;27: 197–213. doi:10.1016/S0168-6445(03)00049-4

5. Hofmann L, Hirsch M, Ruthstein S. Advances in Understanding of the Copper Homeostasis in Pseudomonas aeruginosa. IJMS. 2021;22: 2050. doi:10.3390/ijms22042050

6. Stock AM, Robinson VL, Goudreau PN. Two-Component Signal Transduction. Annu Rev Biochem. 2000;69: 183–215. doi:10.1146/annurev.biochem.69.1.183

7. Zschiedrich CP, Keidel V, Szurmant H. Molecular Mechanisms of Two-Component Signal Transduction. Journal of Molecular Biology. 2016;428: 3752–3775. doi:10.1016/j.jmb.2016.08.003

8. Groisman EA. Feedback Control of Two-Component Regulatory Systems. Annu Rev Microbiol. 2016;70: 103–124. doi:10.1146/annurev-micro-102215-095331

9. Hyre A, Casanova-Hampton K, Subashchandrabose S. Copper Homeostatic Mechanisms and Their Role in the Virulence of Escherichia coli and Salmonella enterica. EcoSal Plus. 2021;9: eESP-0014-2020. doi:10.1128/ecosalplus.ESP-0014-2020

10. Virieux-Petit M, Hammer-Dedet F, Aujoulat F, Jumas-Bilak E, Romano-Bertrand S. From Copper Tolerance to Resistance in Pseudomonas aeruginosa towards Patho-Adaptation and Hospital Success. Genes. 2022;13: 301. doi:10.3390/genes13020301

11. Jeanvoine A, Meunier A, Puja H, Bertrand X, Valot B, Hocquet D. Contamination of a hospital plumbing system by persister cells of a copper-tolerant high-risk clone of Pseudomonas aeruginosa. Water Research. 2019;157: 579–586. doi:10.1016/j.watres.2019.04.011

12. Baker-Austin C, Wright MS, Stepanauskas R, McArthur JV. Co-selection of antibiotic and metal resistance. Trends in Microbiology. 2006;14: 176–182. doi:10.1016/j.tim.2006.02.006

13. Staehlin BM, Gibbons JG, Rokas A, O'Halloran TV, Slot JC. Evolution of a heavy metal homeostasis/resistance island reflects increasing copper stress in Enterobacteria. Genome Biol Evol. 2016; evw031. doi:10.1093/gbe/evw031

14. Chalmers G, Rozas K, Amachawadi R, Scott H, Norman K, Nagaraja T, et al. Distribution of the pco Gene Cluster and Associated Genetic Determinants among Swine Escherichia coli from a Controlled Feeding Trial. Genes. 2018;9: 504. doi:10.3390/genes9100504

15. Arai N, Sekizuka T, Tamamura Y, Kusumoto M, Hinenoya A, Yamasaki S, et al. *Salmonella* Genomic Island 3 Is an Integrative and Conjugative Element and Contributes to Copper and Arsenic Tolerance of *Salmonella enterica*. Antimicrob Agents Chemother. 2019;63: e00429-19. doi:10.1128/AAC.00429-19

16. Klockgether J, Tummler B. Recent advances in understanding Pseudomonas aeruginosa as a pathogen. F1000Res. 2017;6: 1261. doi:10.12688/f1000research.10506.1

17. Grace A, Sahu R, Owen DR, Dennis VA. Pseudomonas aeruginosa reference strains PAO1 and PA14: A genomic, phenotypic, and therapeutic review. Front Microbiol. 2022;13: 1023523. doi:10.3389/fmicb.2022.1023523

18. Schwan WR, Warrener P, Keunz E, Kendall Stover C, Folger KR. Mutations in the cueA gene encoding a copper homeostasis P-type ATPase reduce the pathogenicity of Pseudomonas aeruginosa in mice. International Journal of Medical Microbiology. 2005;295: 237–242. doi:10.1016/j.ijmm.2005.05.005

19. Quintana J, Novoa-Aponte L, Argüello JM. Copper homeostasis networks in the bacterium Pseudomonas aeruginosa. Journal of Biological Chemistry. 2017;292: 15691–15704. doi:10.1074/jbc.M117.804492

20. Teitzel GM, Geddie A, De Long SK, Kirisits MJ, Whiteley M, Parsek MR. Survival and Growth in the Presence of Elevated Copper: Transcriptional Profiling of Copper-Stressed *Pseudomonas aeruginosa*. J Bacteriol. 2006;188: 7242–7256. doi:10.1128/JB.00837-06

21. Turner KH, Everett J, Trivedi U, Rumbaugh KP, Whiteley M. Requirements for Pseudomonas aeruginosa Acute Burn and Chronic Surgical Wound Infection. Garsin DA, editor. PLoS Genet. 2014;10: e1004518. doi:10.1371/journal.pgen.1004518

22. Yu L, Cao Q, Chen W, Yang N, Yang C-G, Ji Q, et al. A novel copper-sensing two-component system for inducing Dsb gene expression in bacteria. Science Bulletin. 2022;67: 198–212. doi:10.1016/j.scib.2021.03.003

23. Kos VN, Déraspe M, McLaughlin RE, Whiteaker JD, Roy PH, Alm RA, et al. The Resistome of Pseudomonas aeruginosa in Relationship to Phenotypic Susceptibility. Antimicrob Agents Chemother. 2015;59: 427–436. doi:10.1128/AAC.03954-14

24. Roy PH, Tetu SG, Larouche A, Elbourne L, Tremblay S, Ren Q, et al. Complete Genome Sequence of the Multiresistant Taxonomic Outlier Pseudomonas aeruginosa PA7. Ahmed N, editor. PLoS ONE. 2010;5: e8842. doi:10.1371/journal.pone.0008842

25. Rudra B, Duncan L, Shah AJ, Shah HN, Gupta RS. Phylogenomic and comparative genomic studies robustly demarcate two distinct clades of Pseudomonas aeruginosa strains: proposal to transfer the strains from an outlier clade to a novel species Pseudomonas paraeruginosa sp. nov. International Journal of Systematic and Evolutionary Microbiology. 2022;72. doi:10.1099/ijsem.0.005542

26. Ng SP. The Heavy Metal Tolerant Soil Bacterium Achromobacter sp. AO22 Contains a Unique Copper Homeostasis Locus and Two mer Operons. J Microbiol Biotechnol. 2012;22: 742–753. doi:10.4014/jmb.1111.11042

27. Winsor GL, Griffiths EJ, Lo R, Dhillon BK, Shay JA, Brinkman FSL. Enhanced annotations and features for comparing thousands of *Pseudomonas* genomes in the Pseudomonas genome database. Nucleic Acids Res. 2016;44: D646–D653. doi:10.1093/nar/gkv1227

28. Trouillon J, Imbert L, Villard A-M, Vernet T, Attrée I, Elsen S. Determination of the two-component systems regulatory network reveals core and accessory regulations across *Pseudomonas aeruginosa* lineages. Nucleic Acids Research. 2021;49: 11476–11490. doi:10.1093/nar/gkab928

29. Hyre AN, Kavanagh K, Kock ND, Donati GL, Subashchandrabose S. Copper Is a Host Effector Mobilized to Urine during Urinary Tract Infection To Impair Bacterial Colonization. Bäumler AJ, editor. Infect Immun. 2017;85: e01041-16. doi:10.1128/IAI.01041-16

30. Bertrand RL. Lag Phase Is a Dynamic, Organized, Adaptive, and Evolvable Period That Prepares Bacteria for Cell Division. Margolin W, editor. J Bacteriol. 2019;201. doi:10.1128/JB.00697-18

31. Irawati W, Djojo ES, Kusumawati L, Yuwono T, Pinontoan R. Optimizing Bioremediation: Elucidating Copper Accumulation Mechanisms of Acinetobacter sp. IrC2 Isolated From an

819 Industrial Waste Treatment Center. Front Microbiol. 2021;12: 713812.
820 doi:10.3389/fmicb.2021.713812

821 32. Fan K, Cao Q, Lan L. Genome-Wide Mapping Reveals Complex Regulatory Activities of BfmR in
822 Pseudomonas aeruginosa. Microorganisms. 2021;9: 485. doi:10.3390/microorganisms9030485

823 33. Ducret V, Gonzalez D, Perron K. Zinc homeostasis in Pseudomonas. Biometals. 2022.
824 doi:10.1007/s10534-022-00475-5

825 34. Novoa-Aponte L, Xu C, Soncini FC, Argüello JM. The Two-Component System CopRS Maintains
826 Subfemtomolar Levels of Free Copper in the Periplasm of Pseudomonas aeruginosa Using a
827 Phosphatase-Based Mechanism. Ellermeier CD, editor. mSphere. 2020;5: e01193-20.
828 doi:10.1128/mSphere.01193-20

829 35. Kung VL, Ozer EA, Hauser AR. The Accessory Genome of *Pseudomonas aeruginosa*. Microbiol
830 Mol Biol Rev. 2010;74: 621–641. doi:10.1128/MMBR.00027-10

831 36. Johnson CM, Grossman AD. Integrative and Conjugative Elements (ICEs): What They Do and
832 How They Work. Annu Rev Genet. 2015;49: 577–601. doi:10.1146/annurev-genet-112414-
833 055018

834 37. Garcillán-Barcia MP, Francia MV, de La Cruz F. The diversity of conjugative relaxases and its
835 application in plasmid classification. FEMS Microbiol Rev. 2009;33: 657–687.
836 doi:10.1111/j.1574-6976.2009.00168.x

837 38. Guglielmini J, Quintais L, Garcillán-Barcia MP, de la Cruz F, Rocha EPC. The Repertoire of ICE in
838 Prokaryotes Underscores the Unity, Diversity, and Ubiquity of Conjugation. Casadesús J, editor.
839 PLoS Genet. 2011;7: e1002222. doi:10.1371/journal.pgen.1002222

840 39. Pal C, Bengtsson-Palme J, Kristiansson E, Larsson DGJ. Co-occurrence of resistance genes to
841 antibiotics, biocides and metals reveals novel insights into their co-selection potential. BMC
842 Genomics. 2015;16: 964. doi:10.1186/s12864-015-2153-5

843 40. Freschi L, Vincent AT, Jeukens J, Emond-Rheault JG, Kukavica-Ibrulj I, Dupont MJ, et al. The
844 Pseudomonas aeruginosa Pan-Genome Provides New Insights on Its Population Structure,
845 Horizontal Gene Transfer, and Pathogenicity. Genome Biol Evol. 2019;11: 109–120.
846 doi:10.1093/gbe/evy259 5215156 [pii]

847 41. Purves J, Thomas J, Riboldi GP, Zapotoczna M, Tarrant E, Andrew PW, et al. A horizontally gene
848 transferred copper resistance locus confers hyper-resistance to antibacterial copper toxicity
849 and enables survival of community acquired methicillin resistant *Staphylococcus aureus*
850 USA300 in macrophages: *Staphylococcus aureus* copper resistance and innate immunity.
851 Environ Microbiol. 2018;20: 1576–1589. doi:10.1111/1462-2920.14088

852 42. Munson GP, Lam DL, Outten FW, O'Halloran TV. Identification of a Copper-Responsive Two-
853 Component System on the Chromosome of *Escherichia coli* K-12. J Bacteriol. 2000;182: 5864–
854 5871. doi:10.1128/JB.182.20.5864-5871.2000

855 43. Baker J, Sengupta M, Jayaswal RK, Morrissey JA. The Staphylococcus aureus CsoR regulates
856 both chromosomal and plasmid-encoded copper resistance mechanisms: Staphylococcus
857 aureus copper resistance and regulation. Environmental Microbiology. 2011;13: 2495–2507.
858 doi:10.1111/j.1462-2920.2011.02522.x

44. Laub MT, Goulian M. Specificity in Two-Component Signal Transduction Pathways. Annu Rev Genet. 2007;41: 121–145. doi:10.1146/annurev.genet.41.042007.170548

45. Yamamoto K, Ishihama A. Transcriptional response of Escherichia coli to external copper: Transcriptional response of E. coli to external copper. Molecular Microbiology. 2005;56: 215–227. doi:10.1111/j.1365-2958.2005.04532.x

46. Gudipaty SA, Larsen AS, Rensing C, McEvoy MM. Regulation of Cu(I)/Ag(I) efflux genes in Escherichia coli by the sensor kinase CusS. FEMS Microbiol Lett. 2012;330: 30–37. doi:10.1111/j.1574-6968.2012.02529.x

47. Gudipaty SA, McEvoy MM. The histidine kinase CusS senses silver ions through direct binding by its sensor domain. Biochimica et Biophysica Acta (BBA) - Proteins and Proteomics. 2014;1844: 1656–1661. doi:10.1016/j.bbapap.2014.06.001

48. Agrawal R, Pandey A, Rajankar MP, Dixit NM, Saini DK. The two-component signalling networks of *Mycobacterium tuberculosis* display extensive cross-talk *in vitro*. Biochemical Journal. 2015;469: 121–134. doi:10.1042/BJ20150268

49. Vemparala B, Valiya Parambathu A, Saini DK, Dixit NM. An Evolutionary Paradigm Favoring Cross Talk between Bacterial Two-Component Signaling Systems. mSystems. 2022;7: e0029822. doi:10.1128/msystems.00298-22

50. Siryaporn A, Goulian M. Cross-talk suppression between the CpxA-CpxR and EnvZ-OmpR two-component systems in *E. coli*. Molecular Microbiology. 2008;70: 494–506. doi:10.1111/j.1365-2958.2008.06426.x

51. Chen Y-T, Chang HY, Lu CL, Peng H-L. Evolutionary Analysis of the Two-Component Systems in Pseudomonas aeruginosa PAO1. J Mol Evol. 2004;59: 725–737. doi:10.1007/s00239-004-2663-2

52. Ranjitkar S, Jones AK, Mostafavi M, Zwirko Z, Iartchouk O, Barnes SW, et al. Target (MexB)- and Efflux-Based Mechanisms Decreasing the Effectiveness of the Efflux Pump Inhibitor D13-9001 in *Pseudomonas aeruginosa* PAO1: Uncovering a New Role for MexMN-OprM in Efflux of β-Lactams and a Novel Regulatory Circuit (MmnRS) Controlling MexMN Expression. Antimicrob Agents Chemother. 2019;63: e01718-18. doi:10.1128/AAC.01718-18

53. Garber ME, Rajeev L, Kazakov AE, Trinh J, Masuno D, Thompson MG, et al. Multiple signaling systems target a core set of transition metal homeostasis genes using similar binding motifs: Multiple signaling systems. Molecular Microbiology. 2018;107: 704–717. doi:10.1111/mmi.13909

54. Ohashi K. Molecular Basis for Promoter Selectivity of the Transcriptional Activator OmpR of Escherichia coli: Isolation of Mutants That Can Activate the Non-Cognate kdpABC Promoter. Journal of Biochemistry. 2005;137: 51–59. doi:10.1093/jb/mvi006

55. Capra EJ, Laub MT. Evolution of Two-Component Signal Transduction Systems. Annu Rev Microbiol. 2012;66: 325–347. doi:10.1146/annurev-micro-092611-150039

56. Wagner D, Maser J, Lai B, Cai Z, Barry CE, Höner zu Bentrup K, et al. Elemental Analysis of *Mycobacterium avium* -, *Mycobacterium tuberculosis* -, and *Mycobacterium smegmatis* - Containing Phagosomes Indicates Pathogen-Induced Microenvironments within the Host Cell's Endosomal System. The Journal of Immunology. 2005;174: 1491–1500. doi:10.4049/jimmunol.174.3.1491

900 57. Caille O, Rossier C, Perron K. A Copper-Activated Two-Component System Interacts with Zinc
901 and Imipenem Resistance in *Pseudomonas aeruginosa*. J Bacteriol. 2007;189: 4561–4568.
902 doi:10.1128/JB.00095-07

903 58. Ducret V, Abdou M, Goncalves Milho C, Leoni S, Martin--Pelaud O, Sandoz A, et al. Global
904 Analysis of the Zinc Homeostasis Network in Pseudomonas aeruginosa and Its Gene Expression
905 Dynamics. Front Microbiol. 2021;12: 739988. doi:10.3389/fmicb.2021.739988

906 59. Elsen S, Ragno M, Attree I. PtrA Is a Periplasmic Protein Involved in Cu Tolerance in
907 Pseudomonas aeruginosa. J Bacteriol. 2011;193: 3376–3378. doi:10.1128/JB.00159-11

908 60. Li MZ, Elledge SJ. Harnessing homologous recombination in vitro to generate recombinant DNA
909 via SLIC. Nat Methods. 2007;4: 251–256. doi:10.1038/nmeth1010

910 61. Trouillon J, Sentausa E, Ragno M, Robert-Genthon M, Lory S, Attree I, et al. Species-specific
911 recruitment of transcription factors dictates toxin expression. Nucleic Acids Res. 2020;48:
912 2388–2400. doi:10.1093/nar/gkz1232 5700547 [pii]

913 62. Berry A, Han K, Trouillon J, Robert-Genthon M, Ragno M, Lory S, et al. cAMP and Vfr Control
914 Exolysin Expression and Cytotoxicity of Pseudomonas aeruginosa Taxonomic Outliers. J
915 Bacteriol. 2018;200. doi:e00135-18 [pii] 10.1128/JB.00135-18 JB.00135-18 [pii]

916 63. Miller JH. Experiments in molecular genetics. Cold Spring Harbor (N.Y.): Cold Spring Harbor
917 Laboratory; 1977.

918 64. Thibault J, Faudry E, Ebel C, Attree I, Elsen S. Anti-activator ExsD Forms a 1:1 Complex with ExsA
919 to Inhibit Transcription of Type III Secretion Operons. Journal of Biological Chemistry. 2009;284:
920 15762–15770. doi:10.1074/jbc.M109.003533

921 65. Liu M, Li X, Xie Y, Bi D, Sun J, Li J, et al. ICEberg 2.0: an updated database of bacterial integrative
922 and conjugative elements. Nucleic Acids Research. 2019;47: D660–D665.
923 doi:10.1093/nar/gky1123

924 66. Abby SS, Néron B, Ménager H, Touchon M, Rocha EPC. MacSyFinder: A Program to Mine
925 Genomes for Molecular Systems with an Application to CRISPR-Cas Systems. Torres NV, editor.
926 PLoS ONE. 2014;9: e110726. doi:10.1371/journal.pone.0110726

927 67. Mareuil F, Doppelt-Azeroual O, Ménager H. A public Galaxy platform at Pasteur used as an
928 execution engine for web services. 2017 [cited 26 May 2023].
929 doi:10.7490/F1000RESEARCH.1114334.1

930 68. Gilchrist CLM, Chooi Y-H. clinker & clustermap.js: automatic generation of gene cluster
931 comparison figures. Robinson P, editor. Bioinformatics. 2021;37: 2473–2475.
932 doi:10.1093/bioinformatics/btab007

933 69. Altschul SF, Gish W, Miller W, Myers EW, Lipman DJ. Basic local alignment search tool. Journal
934 of Molecular Biology. 1990;215: 403–410. doi:10.1016/S0022-2836(05)80360-2

935 70. Seemann T. Prokka: rapid prokaryotic genome annotation. Bioinformatics. 2014;30: 2068–
936 2069. doi:10.1093/bioinformatics/btu153

71. Page AJ, Cummins CA, Hunt M, Wong VK, Reuter S, Holden MTG, et al. Roary: rapid large-scale prokaryote pan genome analysis. Bioinformatics. 2015;31: 3691–3693. doi:10.1093/bioinformatics/btv421

72. Katoh K, Standley DM. MAFFT Multiple Sequence Alignment Software Version 7: Improvements in Performance and Usability. Molecular Biology and Evolution. 2013;30: 772–780. doi:10.1093/molbev/mst010

73. The Galaxy Community, Afgan E, Nekrutenko A, Grüning BA, Blankenberg D, Goecks J, et al. The Galaxy platform for accessible, reproducible and collaborative biomedical analyses: 2022 update. Nucleic Acids Research. 2022;50: W345–W351. doi:10.1093/nar/gkac247

74. Price MN, Dehal PS, Arkin AP. FastTree 2 – Approximately Maximum-Likelihood Trees for Large Alignments. Poon AFY, editor. PLoS ONE. 2010;5: e9490. doi:10.1371/journal.pone.0009490

75. Letunic I, Bork P. Interactive Tree Of Life (iTOL) v5: an online tool for phylogenetic tree display and annotation. Nucleic Acids Research. 2021;49: W293–W296. doi:10.1093/nar/gkab301

Supporting Information

S1 Fig. Delineation of the *pcoA2* operon.

S2 Fig. Copper resistance of different UTI isolates.

S3 Fig. Copper resistance in rich media.

S4 Fig. CusR, CopR and CzcR targets.

S5 Fig. Effect of lack of IrlR and MmnR on the copper-related locus.

S6 Fig. CusR, CopR and CzcR : three regulators, three different outcomes.

S7 Fig. Models of CopRS and CusRS mechansims and cross-talk.

S8 Fig. Similar copper sensitivity of CusRS and CopRS.

S1 Table. Bacterial strains and plasmids used in this study

S2 Table. Primers used in this study

Fig 1. CusRS is a copper responsive and self-regulated TCS. (A) Genetic organization of the copper-related gene locus identified in strain IHMA87. Blue: copper-resistance genes; Orange: regulatory genes. (B) The *pcoA2-cusR* intergenic sequence, framed by the start codon (colored highlights) of each divergent gene. The -10/-35 sequences of the *cusR* promoter (underlined) were predicted using BPROM. The putative CusR

binding site, the palindromic sequence, is in bold and highlighted in gray, with the summit of the peak identified by previous DAPseq [28] identified by an arrowhead. The mutated sequence (*BSmut*) used in the study is indicated in the inset, with the 4 mutated bases indicated by asterisks. (C) Electrophoretic mobility shift assay of CusR on the *pcoA2-cusR* intergenic region. Up to 75 nM of recombinant His6-CusR protein

were incubated with 0.5 nM Cy5-labeled 60-mer probe for 15 min before electrophoresis. For competition assays, excess unlabeled P*cusR* probe (200 nM, 400-fold) was added to the reaction. Arrowheads indicate the positions of unbound free probes (bottom) and CusR/probe complexes (top). (D, E) β-galactosidase activities of the wild-type IHMA87 strain (WT) and the Δ*cusR* strain harboring the indicated P*cusR-lacZ* (D) and P*pcoA2- lacZ* (E) transcriptional fusions. The different regions studied are illustrated in the left panels. Black rectangles: putative -10/-35 boxes of *cusR* promoter; Gray rectangle: palindromic sequence, with the *BSmut* sequence indicated by an asterisk. Arrow: putative transcription start sites, the arrow is dotted for *pcoA2* as it was not predicted by BPROM. Experiments were performed in triplicate and error bars indicate the SEM.

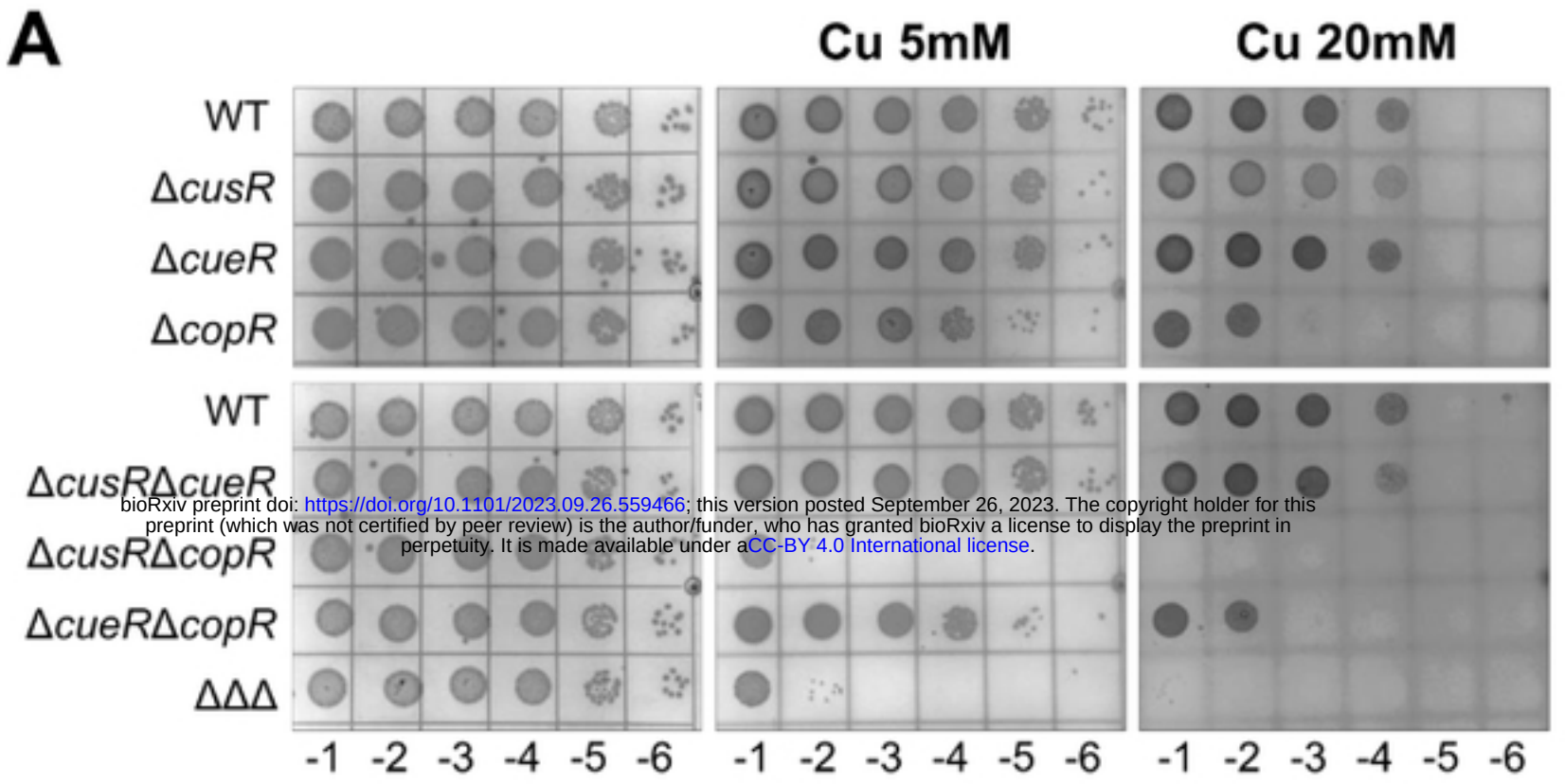

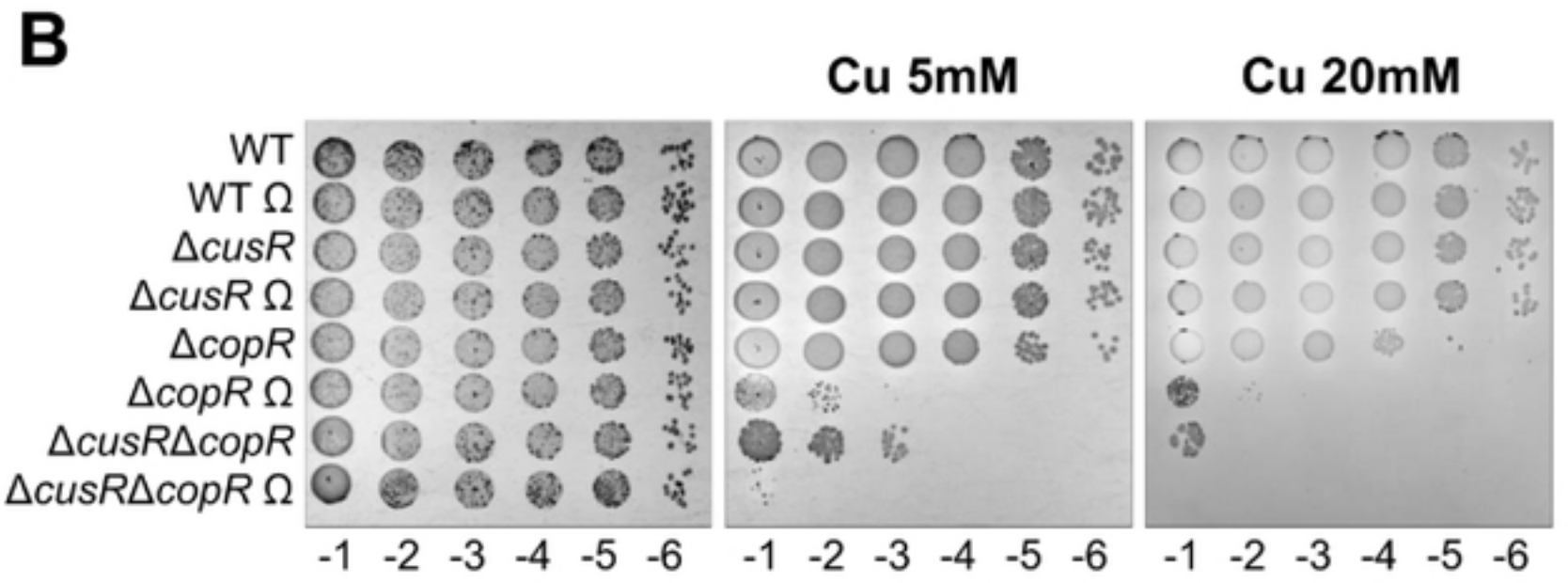

Fig 2. The CusR regulon plays a role in bacterial copper resistance. (A, B) Copper sensitivity plate assays of the different strains used in the study. ΔΔΔ corresponds to the Δ*cusR*Δ*cueR*Δ*copR* triple mutant and Ω to the *pcoA2*::Ω background. 10 µl of 10-fold serial dilutions, as indicated under images (10^{-1} to 10^{-6}), were deposited on M9 plates containing the CuSO4 concentration indicated. Plates were observed after 24 h (M9) or 48 h (Cu) of growth at 37°C.

Fig 3. Cross-regulation by CusRS and CopRS. β-galactosidase activities are shown for strains harboring the P*cusR-lacZ* (A), P*pcoA2-lacZ* (B), P*copA1-lacZ* (C), or P*pcoA-lacZ* (D) transcriptional fusions. ΔΔΔ corresponds to the Δ*cusR*Δ*cueR*Δ*copR* triple mutant. (E) β-galactosidase activities of the wild-type and *pcoA2*::Ω strains containing the indicated transcriptional fusions. Experiments were performed in triplicate; error bars correspond to the SEM.

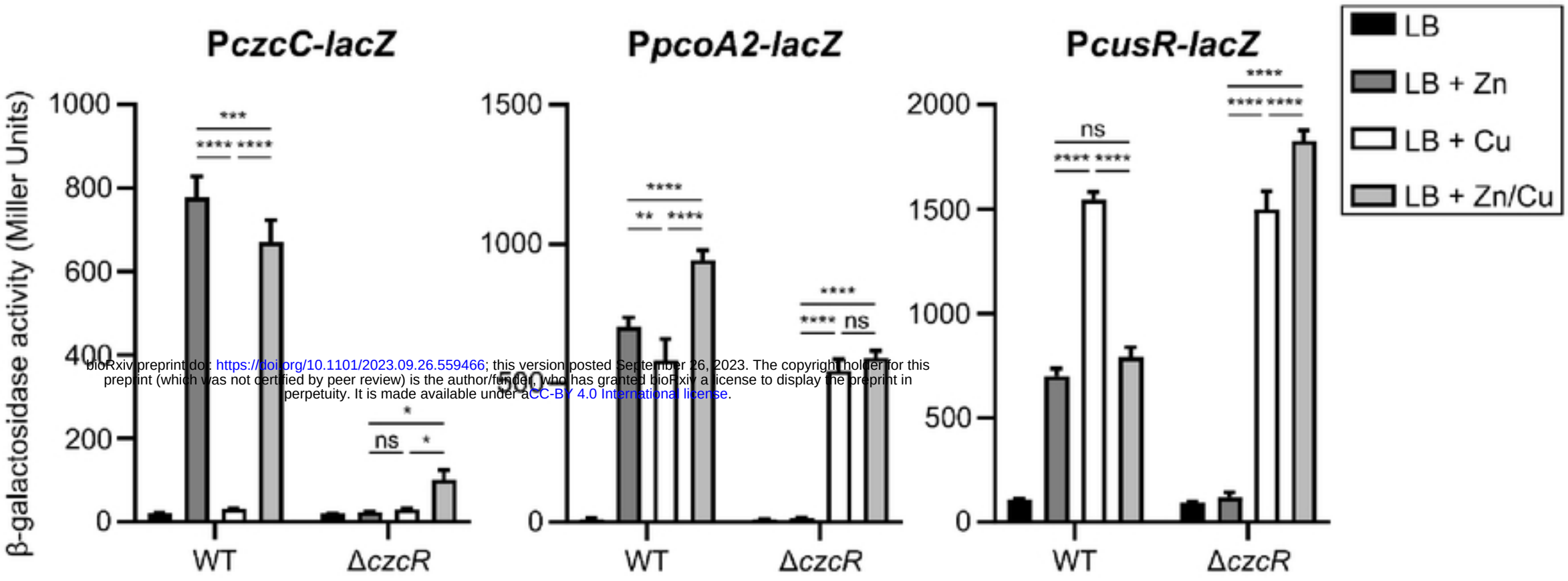

Fig 4. CusRS regulon is also controlled by CzcRS. β-galactosidase activities of the IHMA87 strain (WT) and its isogenic *czcR* mutant harboring the three transcriptional fusions indicated. Activities were measured after 2.5 h of growth in LB or LB supplemented with 0.5 mM $ZnCl_2$, 0.5 mM $CuSO_4$, or 0.5 mM $ZnCl_2$/0.5 mM $CuSO_4$. Error bars indicate the SEM. Statistical significance was assessed by ANOVA, applying Tukey's method (*p*-value, 0.05 [*], 0.01 [**], 0.001 [***], or 0.0001 [****]).

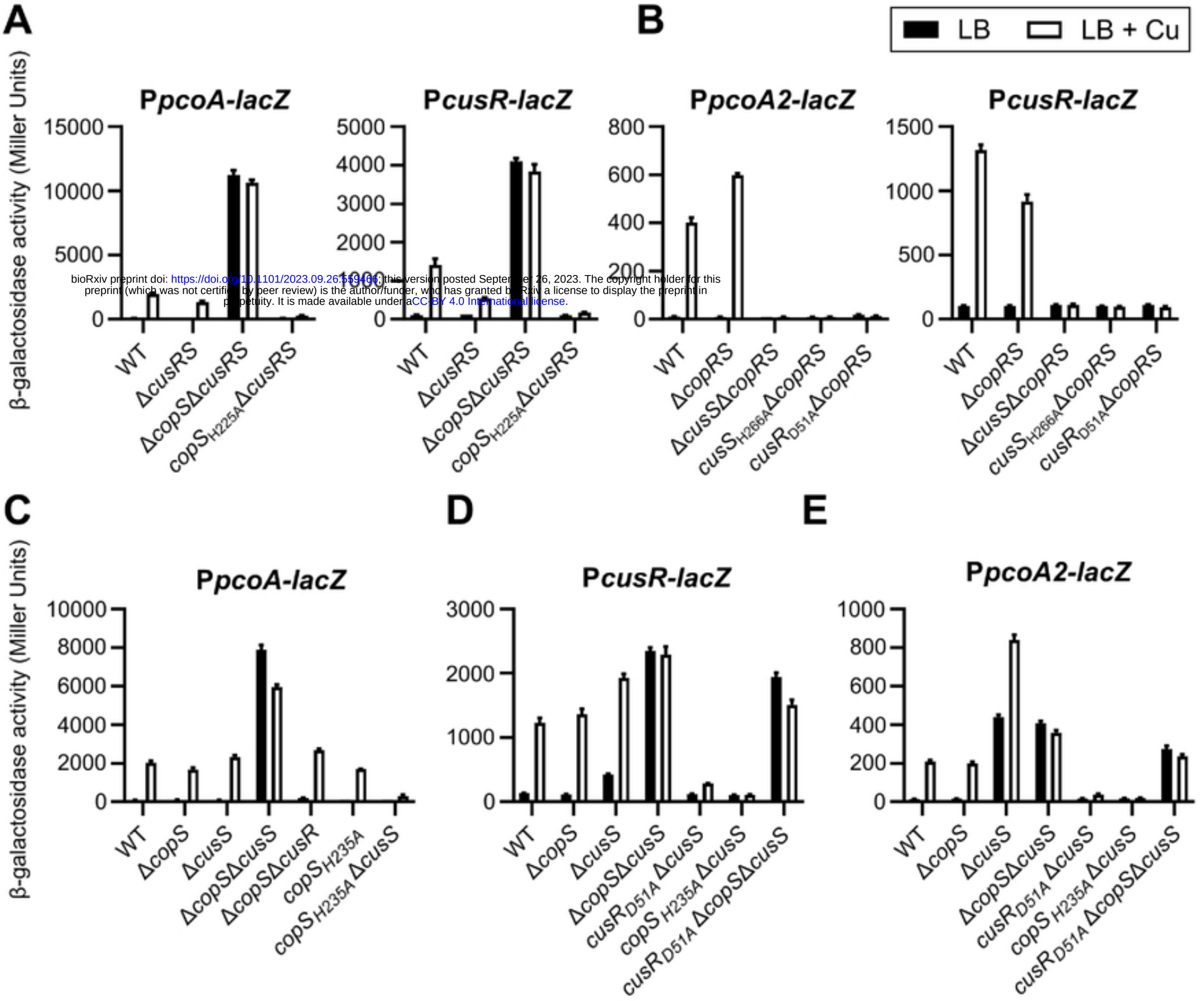

Fig 5. TCS mechanisms and cross-talk. β-galactosidase activities of the strains harboring the transcriptional fusions indicated, after 2.5 h in LB or LB supplemented with 0.5 mM $CuSO_4$. Error bars indicate the SEM.

Fig 6. Conservation of *lysR-cusS* locus *in P. aeruginosa* and *P. paraeruginosa* species. (A) Comparison of the sequences of ICE1_IHMA and PAGI-2. ORFs are color-coded as follows: *pcoA2B2GOFCDK*, blue; *cusRS*, orange; genes involved in conjugation, transfer and integration of ICE, black; homologous genes, white; genes without any corresponding counterparts in ICE1_IHMA and PAGI-2, gray. Intensity of the link

between ORFs was based on % identity between the orthologous proteins. (B) Distribution of genera across genomes harboring modules carried on ICE1_IHMA, as defined in (A). Genera with a single representative are not shown. Module A: *Delftia*, *Diaphorobacter*, *Ralstonia* and *Variovorax*; Module B: *Aerosticca*, *Delftia*, *Tistrella* and *Variovorax*; *lysR-cusS* locus: *Aerosticca*, *Bordetella*, *Delftia*, *Raoultella*, *Ralstonia*, *Tistrella*, *Variovorax* and *Vogesella*. (C) Phylogeny of *P. aeruginosa* and *P. paraeruginosa* species and distribution of *lysR-cusS*. Inset shows unrooted tree at scale, with the number of genomes for each clade The presence of the locus is indicated by blue square, a blue dot signals whether the genes are encoded in a predicted ICE.